

Protein Science

NMR study of the tetrameric KcsA potassium channel in detergent micelles

Jordan H. Chill, John M. Louis, Christopher Miller and Ad Bax

Protein Sci. 2006 15: 684-698; originally published online Mar 7, 2006;
Access the most recent version at doi:[10.1110/ps.051954706](https://doi.org/10.1110/ps.051954706)

References

This article cites 61 articles, 16 of which can be accessed free at:
<http://www.proteinscience.org/cgi/content/full/15/4/684#References>

Article cited in:
<http://www.proteinscience.org/cgi/content/full/15/4/684#otherarticles>

Email alerting service

Receive free email alerts when new articles cite this article - sign up in the box at the top right corner of the article or [click here](#)

Notes

To subscribe to *Protein Science* go to:
<http://www.proteinscience.org/subscriptions/>

NMR study of the tetrameric KcsA potassium channel in detergent micelles

JORDAN H. CHILL,¹ JOHN M. LOUIS,¹ CHRISTOPHER MILLER,² AND AD BAX¹

¹Laboratory of Chemical Physics, NIDDK, National Institutes of Health, Bethesda, Maryland 20892, USA

²Department of Biochemistry, Howard Hughes Medical Institute, Brandeis University, Waltham, Massachusetts 02454, USA

(RECEIVED November 6, 2005; FINAL REVISION January 5, 2006; ACCEPTED January 5, 2006)

Abstract

Nuclear magnetic resonance (NMR) studies of large membrane-associated proteins are limited by the difficulties in preparation of stable protein–detergent mixed micelles and by line broadening, which is typical of these macroassemblies. We have used the 68-kDa homotetrameric KcsA, a thermostable N-terminal deletion mutant of a bacterial potassium channel from *Streptomyces lividans*, as a model system for applying NMR methods to membrane proteins. Optimization of measurement conditions enabled us to perform the backbone assignment of KcsA in SDS micelles and establish its secondary structure, which was found to closely agree with the KcsA crystal structure. The C-terminal cytoplasmic domain, absent in the original structure, contains a 14-residue helix that could participate in tetramerization by forming an intersubunit four-helix bundle. A quantitative estimate of cross-relaxation between detergent and KcsA backbone amide protons, together with relaxation and light scattering data, suggests SDS–KcsA mixed micelles form an oblate spheroid with ~180 SDS molecules per channel. K⁺ ions bind to the micelle-solubilized channel with a K_D of 3 ± 0.5 mM, resulting in chemical shift changes in the selectivity filter. Related pH-induced changes in chemical shift along the “outer” transmembrane helix and the cytoplasmic membrane interface hint at a possible structural explanation for the observed pH-gating of the potassium channel.

Keywords: backbone assignment; detergent; global fold; membrane protein; NMR; NOE; potassium channel; secondary chemical shifts

The potassium channel family is a class of membrane-embedded proteins found in nearly all types of organisms (Miller 2000). Potassium channels are responsible

for the selective conduction of K⁺ ions across cellular membranes and are involved in a multitude of biological functions, particularly electrical signaling and neurotransmission (Hille 2001). Three important attributes of these remarkable cellular gatekeepers are high ion throughput, high fidelity in selecting potassium over other common cations, and the ability to open in response to an external signal (Gulbis and Doyle 2004). K⁺ channels throughout the biological universe share a similar structural topology, with much of the exhibited diversity lying in the gating mechanism that controls the opening of the channel (MacKinnon 2003). Two topologically distinct variants of K⁺ channels are known. In the six-transmembrane-helix channels, or voltage-gated (K_v) subtype, the last two helices form the structural core of the aqueous pore, while the first four helices comprise a gating domain (Pongs et al. 1988). The two-

Reprint requests to: Ad Bax, Laboratory of Chemical Physics, Building 5, Room 126 NIDDK, National Institutes of Health, Bethesda, 9000 Rockville Pike, Bethesda, MD 20892, USA; e-mail: bax@nih.gov; fax: (301) 402-0907.

Abbreviations: CD, circular dichroism; DLS, dynamic light scattering; DM, dodecyl maltopyranoside; DPC, dodecylphosphocholine; HMQC, heteronuclear multiple-quantum coherence; HX, hydrogen solvent-exchange rate; KcsA^E, exchangeable domain of KcsA; KcsATM, transmembrane domain of KcsA; MES, 2-[4-morpholino]-ethanesulfonic acid; NOE, nuclear Overhauser effect; NOESY, nuclear Overhauser effect spectroscopy; NMR, nuclear magnetic resonance; SDS, sodium dodecyl sulfate; SDSL, site-directed spin-labeling; TM1(2), helical transmembrane domain 1(2); tr-HSQC, ¹H-¹⁵N transverse relaxation-optimized heteronuclear single-quantum coherence.

Article published online ahead of print. Article and publication date are at <http://www.proteinscience.org/cgi/doi/10.1110/ps.051954706>.

transmembrane-helix, or inwardly rectifying (K_{ir}) subtype, shares the structural pore topology with its voltage-gated counterparts, but lacks the first four helices (Ho et al. 1993).

Several structures of potassium channels have been elucidated in recent years by X-ray crystallography (Doyle et al. 1998; Jiang et al. 2003; Kuo et al. 2003) and electron microscopy (Jiang et al. 2004), revealing the molecular basis of channel function and regulation. The first of these to be solved, the channel from *Streptomyces lividans* (KcsA), is an assembly of four identical membrane subunits characterized by an “inverted teepee” structure exhibiting fourfold symmetry. Each subunit consists of two membrane-spanning helices (TM1 and TM2) connected by a pore domain that includes the pore helix and the well-conserved TVGYG selectivity motif (Heginbotham et al. 1994). The main-chain carbonyl oxygen atoms of this segment form a K^+ -selective “coordination cage” capable of stabilizing K^+ , but not Na^+ , as these lose their hydration shell upon entering the pore. The aqueous pore narrows toward the cytoplasmic side of the membrane, and is lined by the selectivity filter and the TM2 helix of each subunit (Doyle et al. 1998).

The rapidly increasing structural information for K^+ channels has been invaluable in understanding the molecular mechanisms underlying channel selectivity and high throughput (Gulbis and Doyle 2004). These crystal structures provide high-resolution “snapshots” of the channel in multiple states, but important questions remain regarding the precise dynamic processes underlying the gating mechanism. To date, most studies have focused on the transmembrane and pore regions, whereas the N- and C-terminal domains, which typically exhibit insufficient electron density, appear unstructured or were excised for obtaining high-quality crystals. These cytoplasmic domains have been implicated in mediating the formation of channel tetramers and pH-dependent gating (Cortes et al. 2001; Molina et al. 2004). For these reasons, structural studies of full-length KcsA that address dynamic issues at the molecular level should enhance our understanding of potassium channel function.

Nuclear magnetic resonance (NMR) has evolved in recent years into an important tool for studying the structure and dynamics of proteins in solution (Ferentz and Wagner 2000; Wider 2005). Several key methodological advances have allowed NMR to address soluble proteins of increasing size and complexity (Bax and Grzesiek 1993; Pervushin et al. 1997; Salzmann et al. 1998; Riek et al. 2002; Tugarinov et al. 2002; Frueh et al. 2005). As membrane-associated proteins play pivotal roles in a wide range of biological processes, application of NMR methods to the study of such systems has been

a prime objective. Solid-state NMR methods have been used to study membrane peptides and small proteins, particularly transmembrane helical domains (Fu and Cross 1999; Marassi and Opella 1999; Mesleh et al. 2003). High-resolution NMR studies have afforded several structures of proteins in the 15–30 kDa range (Arora et al. 2001; Hwang et al. 2002; Fernández and Wüthrich 2003; Oxenoid and Chou 2005). However, large (>30 kDa) membrane-associated proteins continue to present a formidable challenge in NMR studies. These highly hydrophobic proteins must be sequestered from the aqueous environment in relatively fluid macromolecular lipid or detergent assemblies. As a result, samples are prone both to line broadening due to exchange processes as well as aggregation. Furthermore, such protein–detergent systems rapidly reach the limit at which long tumbling times preclude the acquisition of meaningful NMR data (Arora and Tamm 2001). This is particularly true for helical proteins, for which spectral dispersion is typically poor. Clearly, NMR methods suitable for the study of large membrane proteins must be established if it is to remain relevant for structural investigation of membrane-associated systems.

These considerations motivated us to examine the KcsA tetramer as a model system for developing NMR methods that bring relatively large helical transmembrane systems within the reach of solution NMR. Considering that it can be expressed and purified in sufficient quantities, is suitable for isotopic labeling, and possesses high thermostability, KcsA represents an attractive system for this purpose. In addition, NMR is well suited for probing dynamic processes and also provides access to the terminal regions of the KcsA chain, which may play an important role in tetramerization and regulation of ion conductance. By surveying samples of KcsA solubilized in various detergent micelles, we established that sodium dodecyl sulfate (SDS) micelles containing the homotetrameric 68-kDa channel were amenable to backbone assignment. The secondary structure of KcsA determined by secondary chemical shifts and hydrogen-exchange protection factors closely agrees with the KcsA crystal structure, and indicates the presence of a relatively long α -helix in the C-terminal cytoplasmic domain. Quantitative cross-relaxation attenuation experiments have been used to map interactions between detergent and protein, and results indicate that the detergent forms a hemitoroid around the membrane-spanning hydrophobic domains of the channel. The KcsA channel in SDS micelles exhibits K^+ -induced chemical shift changes in selectivity filter, indicating that the channel maintains its biological activity under these conditions. Correlated pH-induced changes observed for both TM domains suggest a possible role for an intersubunit interaction in the pH-gating of the channel.

Results

Characterization of KcsA in SDS micelles

A critical step toward the study of KcsA by NMR was establishing conditions at which high-quality NMR data could be acquired. KcsA, throughout this work, refers to residues 16–160 of the channel, beginning with the N-terminal segment $^{16}\text{LLGR}^{20}\text{H}$ and ending with the C-terminal segment $^{156}\text{DDNR}^{160}\text{R}$. This deletion mutant, lacking the first 14 N-terminal residues of full-length KcsA, was found to have increased thermostability (M. Lawrence and C. Miller, unpubl.). Samples of tetrameric KcsA in various detergent micelles were prepared by purifying dodecyl maltopyranoside (DM)-solubilized protein on a size-exclusion column equilibrated with a buffer containing the appropriate detergent (Takeuchi et al. 2003). Our survey of detergents concluded that the micelles formed by the anionic SDS were best suited for this purpose. NMR samples containing 0.25–0.35 mM of tetrameric KcsA and a 400- to 800-fold excess of SDS at 323 K allowed the acquisition of triple-resonance NMR data amenable to backbone assignment. Despite extensive efforts, data of comparable quality could not be obtained in other detergents, in which, typically, only signals emanating from flexible, unstructured residues could be observed.

As has been reported previously for KcsA in various detergent micelles (Heginbotham et al. 1997; Molina et al. 2004), KcsA in SDS micelles behaves as a highly stable molecular ensemble. It migrates as a tetramer in con-

ventional SDS-PAGE even after exposure to elevated temperatures (75°C for 60 min), pH 10 or 4 M urea. Dynamic light scattering (DLS) measurements indicate a molecular weight of 115 ± 10 kDa for the protein–detergent ensemble, corresponding to an aggregation number of 160 ± 35 SDS molecules per KcsA tetramer (Fig. 1A). Circular dichroism (CD) measurements of KcsA in SDS indicate that it is $\sim 50\%$ helical, and highly similar in helical content to KcsA in dodecylphosphocholine (DPC) and DM micelles (Fig. 1B). DPC has been acknowledged as a suitable membrane surrogate in structural studies (Oxenoid et al. 2004), and DM is a mild and often-used non-ionic detergent for stabilization of membrane proteins. This evidence, together with specific chemical shift changes in the selectivity filter upon addition of K^+ (vide infra), strongly suggests that KcsA in SDS micelles embodies a valid representation of the cellular conformation of the channel.

General approach to backbone assignment of KcsA

As a large protein–detergent assembly, exceeding 100 kDa, backbone assignment of KcsA requires deuteration of all ^{13}C nuclei, while maintaining full protonation in backbone amide sites, without which triple resonance experiments cannot be efficiently acquired (Grzesiek et al. 1993; Tugarinov et al. 2004). This is typically achieved by performing expression in D_2O -based medium, followed by base-catalyzed back-exchange of amide protons during purification. In cases where this is insuffic-

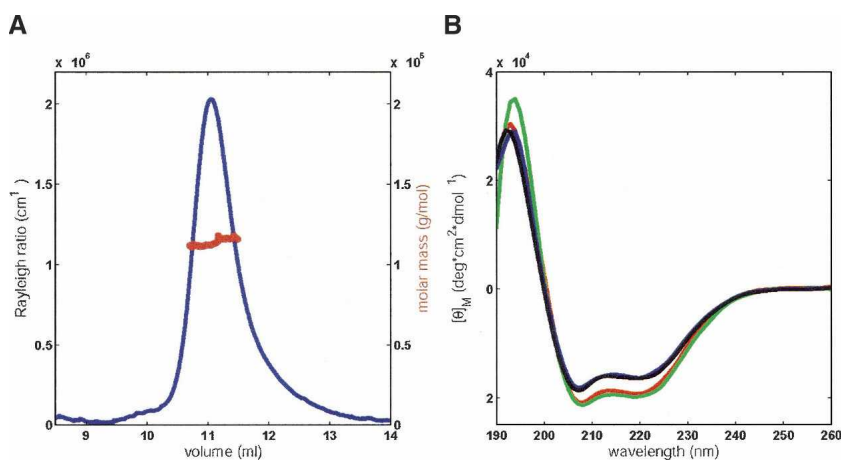


Figure 1. Biophysical characterization of KcsA. (A) Characterization of SDS–KcsA micelles by size-exclusion chromatography in conjunction with dynamic light scattering. The angle-dependent light scattering, proportional to protein concentration, is shown as a function of elution volume in blue. Molar mass values extracted from the analysis of light scattering and refractive index data for SDS–KcsA eluting between 10.7 and 11.5 mL are displayed in red. The estimated weight of the SDS–KcsA micelle is 115 ± 10 kDa. (B) CD spectra of 25 μM samples of tetrameric KcsA in various detergents. Almost identical curves for KcsA in SDS micelles at pH 6.0 and 8.0 are shown in black and blue, respectively. The highly similar curves obtained for KcsA in a 4:1 mix of DPC and SDS, and KcsA in DM are shown in red and green, respectively. Predicted helical contents are 47%, 51%, 57%, and 59% for SDS at pH 6, SDS at pH 8, 4:1 DPC:SDS and DM, respectively.

ient, denaturation and refolding of the protein may be used to obtain full protonation of backbone amide sites (Tugarinov et al. 2004). However, the highly stable KcsA resisted all attempts at back-exchange of amide protons at its detergent-embedded core. As a result, KcsA expressed in D_2O -based medium exhibited only 68% of the expected amide proton cross-peaks. Extended exposure to pH values as high as 10 and temperatures as high as $75^\circ C$, just under its melting point, failed to introduce protons into these well-protected sites. While successful refolding of denatured KcsA into its tetrameric form has been reported (Valiyaveetil et al. 2002), in our hands, the overall yield of this process remains insufficient for preparation of NMR samples.

We resolved this difficulty by treating KcsA as a two-domain protein, extending the approach posited by Lohr and coworkers (Lohr et al. 2003). At the basis of this approach lies the assumption that nonexchangeable protons will be heavily clustered along the sequence of KcsA. Accordingly, backbone assignment was performed concurrently for two samples. The first contained 2H , ^{13}C , ^{15}N -labeled KcsA expressed in D_2O -based M9 medium, allowing the assignment of the solvent-accessible (exchangeable) domain of KcsA ($KcsA^E$). The second contained KcsA expressed in glucose-deficient H_2O -based medium supplemented with 2H , ^{13}C , ^{15}N -labeled nutrients. This afforded a 2H ($^1H^\alpha$), U- ^{13}C , ^{15}N -labeled KcsA sample, for which all amide sites were fully protonated, side-chain ^{13}C sites were highly deuterated, and $^{13}C^\alpha$ sites were fractionally deuterated at a level that varied with amino acid type. This sample was lyophilized and reconstituted in D_2O , selectively quenching signals arising from the solvent-accessible domain, and allowing the assignment of the transmembrane, or core domain of KcsA ($KcsA^{TM}$). The 1H , ^{15}N -TROSY-HSQC (tr-HSQC) "fingerprint" regions for the two domains are shown in Figure 2.

Although this approach requires the acquisition of NMR data for both samples, doubling the overall measurement time, these two complementary samples facilitated the assignment process by dividing the data into two self-contained subsets.

Backbone assignment of KcsA

The differences in resonance line width between the $KcsA^E$ and $KcsA^{TM}$ domains (Fig. 2) are striking, and indicate that internal mobility is strongly decreased for protein segments enclosed in the micelle. An average τ_C value of 40 nsec is estimated for the $KcsA^{TM}$ domain on the basis of ^{15}N relaxation measurements, whereas $KcsA^E$ transverse relaxation rates were quite heterogeneous and, on average, about twofold lower, indicative of extensive internal mobility for the $KcsA^E$ domain. These differences in mobility determined the appropriate strategy for backbone assignment of the two domains. In the case of $KcsA^E$, line widths were sufficiently narrow to obtain intra- and inter-residual connectivities for both $^{13}C'$ and $^{13}C^\alpha$ nuclei. Thus, the assignment of its backbone resonances was predominantly based upon correlations of $^{13}C'$ and $^{13}C^\alpha$ nuclei to their adjacent amide protons. In contrast, the broader line widths of $KcsA^{TM}$ rendered the out-and-back three-step transfer experiments tr-HN(CO)CA and tr-HN(CA)CO (Salzmann et al. 1998) inefficient, precluding detection of the inter-residue connectivities. The intrinsically helical character of this domain and its favorable dispersion of peaks in the tr-HSQC spectrum enabled us to complete the assignment utilizing a set of ^{15}N -separated NOESY experiments. This strategy is demonstrated in Figure 3. By independent optimization of the assignment strategy for each domain, an overall assignment level in excess of 97% of native non-proline residues was obtained.

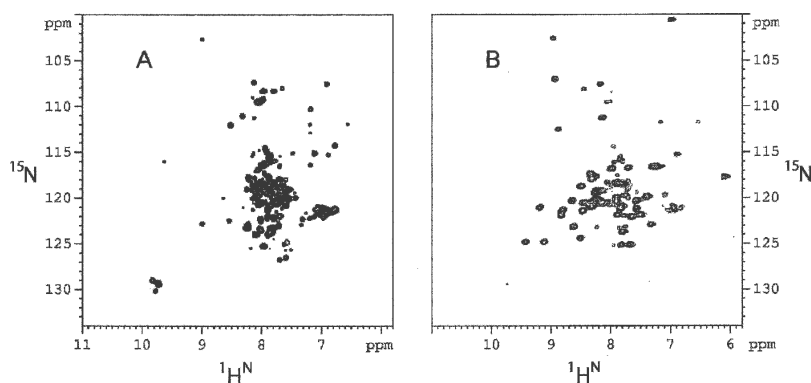


Figure 2. TROSY-HSQC fingerprint regions of the two KcsA domains. 1H - ^{15}N -TROSY-HSQC (tr-HSQC) fingerprint regions of the solvent-accessible domain, $KcsA^E$ (A), and the transmembrane domain, $KcsA^{TM}$ (B). Spectra were acquired using 0.25–0.3 mM samples of tetrameric KcsA samples in 25 mM MES (pH 6.0) and SDS at 400–600:1 excess on a Bruker DRX800 spectrometer equipped with a cryogenic triple-resonance probe. Total acquisition time was 60 (90) min for the $KcsA^E$ ($KcsA^{TM}$) domain.

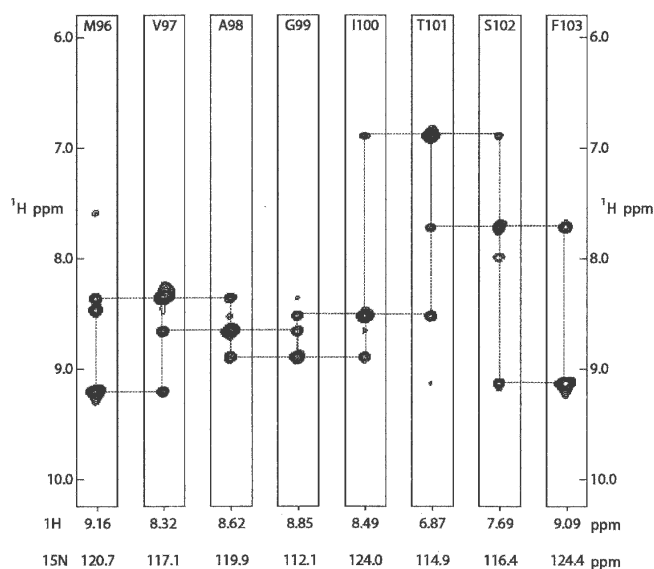


Figure 3. Backbone assignment of KcsATM using inter-residual ¹H^N-¹H^N connectivities. Strips derived from a ¹⁵N-separated NOE-HMQC spectrum of KcsATM exhibit the characteristic helical ¹H^N-¹H^N NOE pattern that facilitated backbone assignment of this domain. Each strip represents a single KcsATM amide proton, with ¹H and ¹⁵N chemical shift resonances shown *below* the strips. Off-diagonal cross-peaks indicate the resonance frequency of the two adjacent amide protons (dotted boxes), indicating the identity of the neighboring residues. This “backbone walk” is demonstrated for residues 96–103 in the TM2 helix. The spectrum was acquired on a Bruker DRX800 spectrometer equipped with a cryogenic triple-resonance probe for a sample of 0.25 mM tetrameric KcsATM in 25 mM MES (pH 6.0), 600:1 excess SDS, and 99% D₂O, using a mixing time of 70 msec.

Figure 4 describes the distribution of KcsA residues between these two domains. The KcsATM domain is characterized by amide protons that remain nonexchangeable, or very slowly exchangeable, over a period

of several weeks in a 99% D₂O sample at pH 6 and 323 K. Protein segments included in KcsATM were residues 35–50, 65–79, and 87–111. The first and third segments roughly correspond to the two transmembrane helices (TM1 and TM2, respectively) in the KcsA structure, and the second overlaps with the pore helix and selectivity filter. All other residues were accessible to solvent, with backbone amide solvent exchange rates in the 0.001–10 sec⁻¹ range, and comprise the KcsA^E domain. Several residues could be observed in both samples, including L35, L49-A50, G79, W87-G88, and T107-A111, corresponding to residues located at the boundaries of the two domains.

The secondary structure of KcsA

Using the well-known correlation between backbone ¹³C chemical shifts and secondary structure, the local backbone structure of KcsA in SDS micelles could be established (Fig. 5). NMR data define four helical segments in KcsA, connected by loops with extended backbone conformation. Strong helical indicators are found for residues 31–52, 62–73, and 86–115, corresponding to the positions of TM1, the pore helix, and TM2, respectively. A fourth helical segment, spanning residues 142–155, represents an additional helix in the C-terminal cytoplasmic domain. The ¹³C chemical shift helical indicators in this helix are structurally and statistically significant, although not as strong as observed for the TM domains. The four KcsA helices are similarly identified and located by an analysis of NOE cross-peaks between adjacent backbone amide protons. The vast majority of residues in the proposed helical sequences exhibit a strong ¹H^N(*i*)-¹H^N(*i* + 1) interaction, which is characteristic in segments with helical structure. The distinction

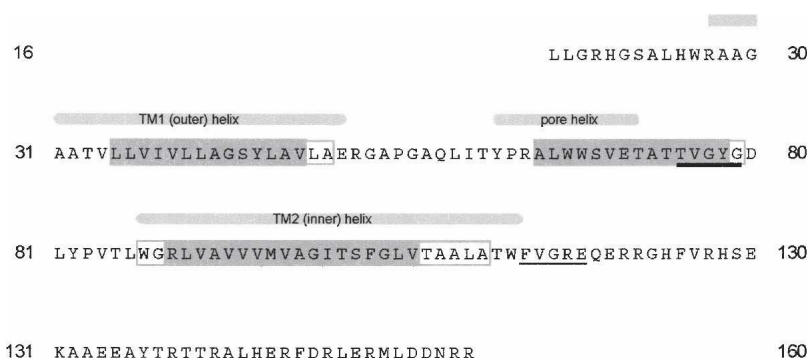


Figure 4. Assignment of KcsA resonances. Shown is the sequence of KcsA^{16–160} used in the current study. Shaded gray residues have amide protons that are inexchangeable or very slowly exchangeable in D₂O, and represent the KcsATM domain. Other residues are solvent accessible and comprise the KcsA^E domain. Residues in open gray rectangles are observed in both samples. Overhead gray bars indicate the two membrane-spanning helices and the pore helix as seen in the crystal structure (Doyle et al. 1998). The selectivity filter (residues 75–79) is heavily underlined, and residues 114–118, exhibiting a large pH-induced change in chemical shift, are lightly underlined. The N-terminal His₆-tag used for purification is omitted for clarity.

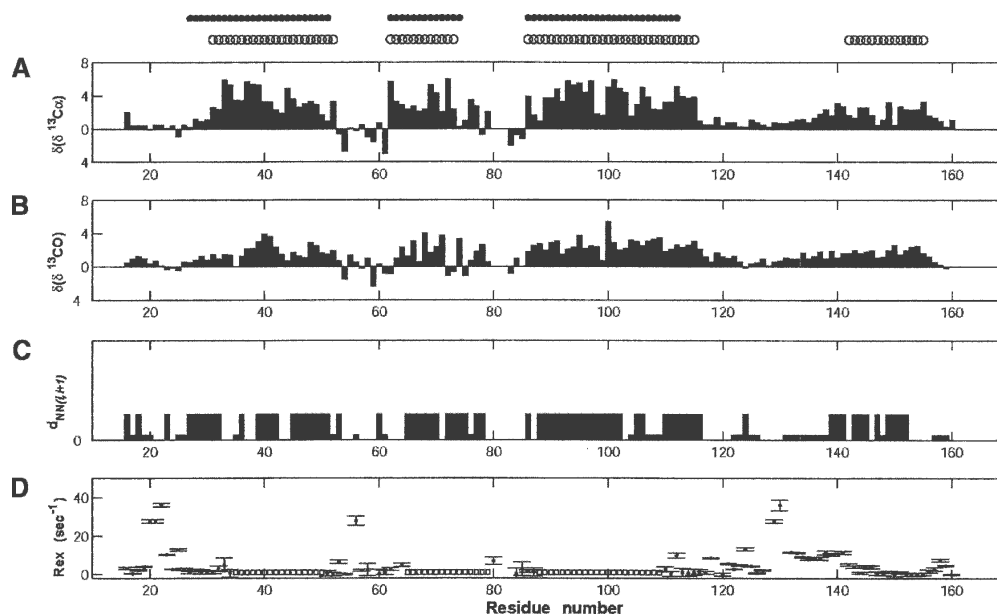


Figure 5. Backbone NMR data predict the secondary structure of KcsA. Deviations of chemical shifts from random coil values (based on Zhang et al. 2003) are shown for $^{13}\text{C}^\alpha$ (A) and $^{13}\text{C}^\gamma$ (B) nuclei along the KcsA backbone. Downfield values (positive deviations) of the ^{13}C resonance indicate a backbone helical conformation. (C) $^1\text{H}^{\text{N}}(i)$ - $^1\text{H}^{\text{N}}(i+1)$ NOE connectivities observed in ^{15}N -separated NOE-HMQC spectra of KcsA. Data from several spectra were combined by measuring ratios between cross-peak and diagonal peak intensities, and classifying these in two categories, corresponding to strong and weak $^1\text{H}^{\text{N}}(i)$ - $^1\text{H}^{\text{N}}(i+1)$ interactions. (D) HX rates of KcsA amide protons. Exchange rates were measured by comparing the intensity of a given tr-HNCO peak acquired at 600 MHz with and without a preceding water-inversion peak. KcsATM protons are considered nonexchangeable on this scale, as designated by the open squares along the axis. No effort was made to exclude the effect of exchangeable-proton-mediated magnetization transfer, which may increase apparent exchange rates. For example, the elevated rate observed for T112 is likely the result of fast exchange of its β -OH proton with solvent, followed by NOE magnetization transfer to its backbone amide. The secondary structure elements in the crystal structure (Doyle et al. 1998) and as determined by NMR are shown *above* in filled and open circles, respectively.

between structured and disordered segments in the C-terminal domain (residues 121–160) is particularly striking. The total helical content of KcsA as determined by NMR (78 of 152 residues) is consistent with the results of CD measurements (Fig. 1B).

Rates of exchange of amide protons with the solvent (HX rates) have been extensively used as a measure of secondary structure in proteins (Wand and Englander 1996; Maity et al. 2003). These were quantitatively derived for the KcsA^E domain by comparing the amide proton intensities observed with and without selective inversion of the H_2O resonance prior to acquisition of a 3D-TROSY-HNCO (tr-HNCO) spectrum. At pH 8.0, residues 121–135 and 142–155 have average exchange rates of 10.5 (maximum of 36) and 1.5 (maximum of 5) sec^{-1} , suggesting the presence of a helix in the latter segment. Similarly, the four N-terminal residues of KcsA (16–19) and the next six residues (20–25) average an exchange rate of 2.4 (maximum of 3.9) and 19.5 (maximum of 36) sec^{-1} , respectively. In these segments the large increase in hydrogen exchange rate of G21 over that of G18 is particularly striking (Fig. 5). Consistent

with secondary shift data, this suggests the existence of an additional helix in the N-terminal domain, the majority of which is excluded from the construct used for this work.

Protein–detergent interactions

Having analyzed the secondary chemical shifts in KcsA, we turn our focus to the assembly of detergent molecules, which surround it and stabilize it in aqueous solution. By measuring dipole–dipole cross-relaxation between detergent and protein backbone amide protons, NMR can characterize the spatial organization of micelle-solubilized KcsA. Considering that identification of individual backbone amides required three-dimensional dispersion of the signals in a tr-HNCO spectrum, we opted for a set of selective SDS inversion experiments to probe the NOE interaction between SDS and KcsA, rather than extending the three-dimensional experiment to four dimensions, or resorting to reduced-dimensionality experiments. The selective NOE measurements are carried out by inverting individual SDS resonances prior to acquisition of the

3D-tr-HNCO data set. Inversion pulses afforded a 70%–80% inversion of the selected detergent proton, whereas its effect upon nonexcited SDS protons was minimal. The NOE-related attenuation during a mixing time of 250 msec was measured as the ratio between the intensities associated with a given tr-HNCO signal in spectra recorded in interleaved fashion with and without the inversion pulse.

The ^1H SDS spectrum exhibits four signals, corresponding to the C^1H_2 , C^2H_2 , $\text{C}^{3-11}\text{H}_2$, and C^{12}H_3 protons, resonating at 3.8, 1.5, 1.25 (broad), and 0.85 ppm, respectively. Results from the experiment involving inversion of the downfield protons are difficult to interpret due to overlap with non-negligible levels of C^α protonation in KcsA^{TM} , thereby giving rise to strong intraprotein NOEs. The results for selective inversion of each of the three upfield SDS protons are summarized in Figure 6. Overall, only moderate attenuation of the H^{N} magnetization, even after 250 msec, is observed. As expected, the protein–detergent interaction is strongest for membrane-buried domains, exhibiting maximum NOE attenuations of 15%, 30%, and 15%, for inversion of the C^2H_2 , $\text{C}^{3-11}\text{H}_2$, and C^{12}H_3 protons, respectively. The protein–detergent interactions observed for the “outer” and “inner” transmembrane helices (TM1 and TM2, respectively) are comparable. In contrast, the entire C-terminal domain (residues 121–160) is hardly affected by inversion of detergent protons, indicating that few, if

any, micellar interactions exist for this domain. Notably, NOE attenuation increases at the N-terminal residues 16–19, particularly when compared with the C-terminal segment. Interactions between these residues and the detergent hint once again at the existence of a membrane-embedded N-terminal helix in full-length KcsA .

A comparison between attenuation maps for different types of SDS protons is revealing. Generally speaking, highest attenuation levels are observed for the $\text{C}^{3-11}\text{H}_2$ protons, making them the most sensitive probe of protein–detergent interactions. However, since the overlapping $\text{C}^{3-11}\text{H}_2$ protons span the length of the SDS monomer, the results for the C^{12}H_3 and C^2H_2 protons are used to interpret the relative orientation (in the head-to-tail sense) of the detergent in the protein–micelle assembly. NOE attenuations for the $\text{C}^{3-11}\text{H}_2$ and C^{12}H_3 protons are highly correlated for the TM1 and TM2 helices, whereas for the pore helix it is the attenuations of the $\text{C}^{3-11}\text{H}_2$ and C^2H_2 protons that are correlated. These results are summarized in Figure 7, displaying the results of SDS-inversion experiments juxtaposed upon the structure of KcsA . The attenuation maps for C^2H_2 (Fig. 7A) and C^{12}H_3 (Fig. 7C) protons are highly complementary. Whereas inversion of the SDS-charged headgroups affects KcsA residues at the membrane–solvent interface, inversion of the hydrophobic tails affects residues in the membrane-spanning domain. The selectivity filter appears relatively sheltered

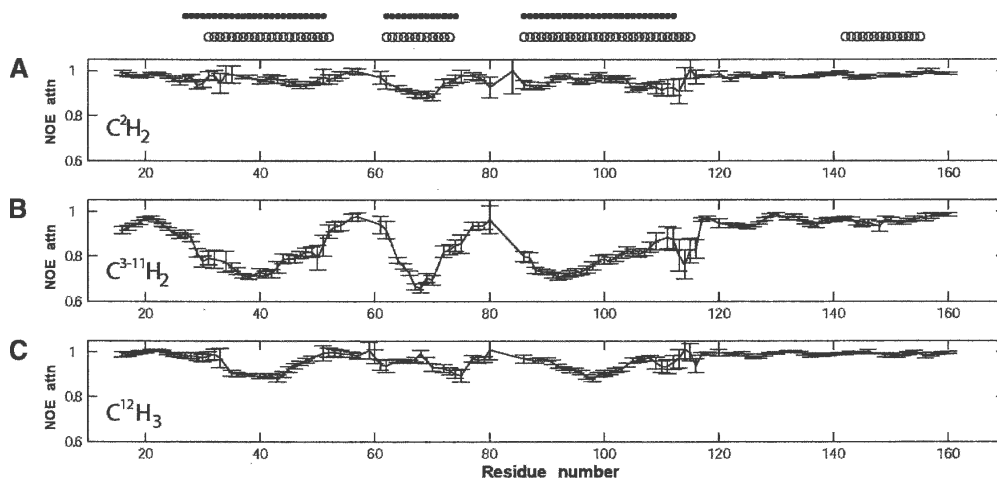


Figure 6. Amide proton attenuation due to intermolecular detergent–protein NOEs. Shown is the ratio of the intensity of a given tr-HNCO correlation in the presence and absence of a selective inversion pulse applied to SDS protons followed by a mixing time of 250 msec. The figure displays attenuations upon inverting the C^2H_2 methylene group, resonating at 1.5 ppm (A), the nine overlapping methylene groups, $\text{C}^{3-11}\text{H}_2$, resonating at 1.25 ppm (B), and the terminal methyl group, C^{12}H_3 , resonating at 0.85 ppm (C). Due to the effective magnetization transfer by intraprotein NOE and in the interests of improved signal-to-noise, a smoothing function was applied to the three curves where each data point represents a weighted average of a triad of amide protons, with all data weighted by the inverse of the experimental error squared, and the center proton doubly weighted with respect to its neighbors. tr-HNCO data were acquired separately for KcsA^{E} and KcsA^{TM} at 600 MHz, with total experimental times of 14 and 60 h, respectively. The secondary structure elements in the crystal structure (Doyle et al. 1998) and as determined by NMR are shown above in filled and open circles, respectively.

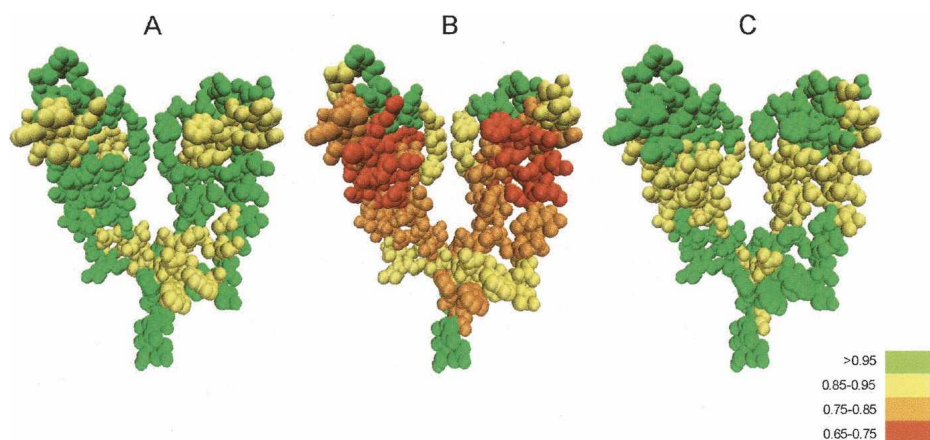


Figure 7. Structural representation of detergent-protein NOE magnetization transfer. The results of the intermolecular NOE experiments for inversion of C^2H_2 protons (A), $C^{3-11}H_2$ protons (B), and $C^{12}H_3$ protons (C) are mapped upon the crystal structure of residues 23–119 of KcsA (Doyle et al. 1998). Only two diametrically opposed subunits of the tetramer are shown for clarity. Residues colored red to green represent a gradual scale of weakening intermolecular interactions.

from detergent NOEs, as expected for this highly buried sequence. With the exception of N-terminal residues 16–19, KcsA segments in the extracellular and cytoplasmic domains are characterized by low attenuation levels in all experiments, thereby clearly demarcating the membrane interface.

K^+ -induced chemical shift changes in the KcsA selectivity filter

The KcsA selectivity filter uses a coordinated array of backbone carbonyl oxygens and side-chain hydroxyl groups of residues $^{75}TVGY^{79}G$ to selectively stabilize incoming K^+ ions as they traverse the membrane (Doyle et al. 1998). Titration of tetrameric KcsA in SDS micelles with KCl affects the chemical shifts of residues $^{73}ATTV^{77}G$, a segment that forms the two “inner” coordination sites (of four) for K^+ . The largest difference is observed for the backbone amide of V76, whose ^{15}N chemical shift changes by about 1.4 ppm (Fig. 8A). Additional residues affected by the presence of K^+ include L41 and A42 of the TM1 helix and A98 of TM2. Overall, the results indicate an equilibrium between K^+ -bound and K^+ -deficient states, which, for conditions at which NMR data were acquired, is governed by a dissociation constant of $K_D \sim 3$ mM (Fig. 8B). For V76, an additional 13 Hz ^{15}N line broadening is observed at the midpoint of the titration relative to the endpoints (Fig. 8A), which, using standard equations for two-site exchange, indicates an exchange rate $k_{ex} \approx 10^4$ s $^{-1}$.

Recently solved channel structures have established that the filter is electrostatically driven to adopt an alternative conformation in the absence of K^+ , and that residue V76 is most affected by this change (Zhou

et al. 2001; Zhou and MacKinnon 2003). Furthermore, comparable K_D values for K^+ high-affinity sites have been reported in previous physiological (LeMasurier et al. 2001) and structural (Zhou and MacKinnon 2003) titration studies. Therefore, our NMR results strongly suggest that the functionality of the channel is preserved in SDS micelles.

pH-induced changes in KcsA

KcsA exhibits pH-dependent gating, shifting to the open state in bilayers when its cytoplasmic face is exposed to pH values below ~ 5 (Cuello et al. 1998; Heginbotham et al. 1999). It is therefore interesting to follow pH-induced changes in KcsA chemical shifts in an attempt to account for this gating mechanism on the molecular level. The KcsA backbone chemical shifts were reassigned for samples in 20 mM Tris (pH 8.0) buffer and compared with values observed in 25 mM MES (pH 6.0). Weighted chemical shift deviations ($\Delta = \sqrt{((\delta_H)^2 + (\delta_N/5)^2)}$) in the tr-HSQC spectra are summarized in Figure 9. Most changes in chemical shift found in the C-terminal cytoplasmic domain can be attributed to local electrostatic effects of charged residues affected by the pH change. An important exception in this regard is the change observed for residues 114–117 at the cytoplasmic end of the TM2 helix. Equally interesting are the smaller, yet significant chemical shift changes in the KcsATM domain, despite its being sheltered from the macroscopic environment by the SDS micelle. Notably, these changes cluster in the TM1 helix; of the eight residues exhibiting the largest chemical shift changes (> 0.07 ppm), and which are unaffected by local electrostatic effects, six are located in this domain. Residue T75 of the selectivity filter shows considerable

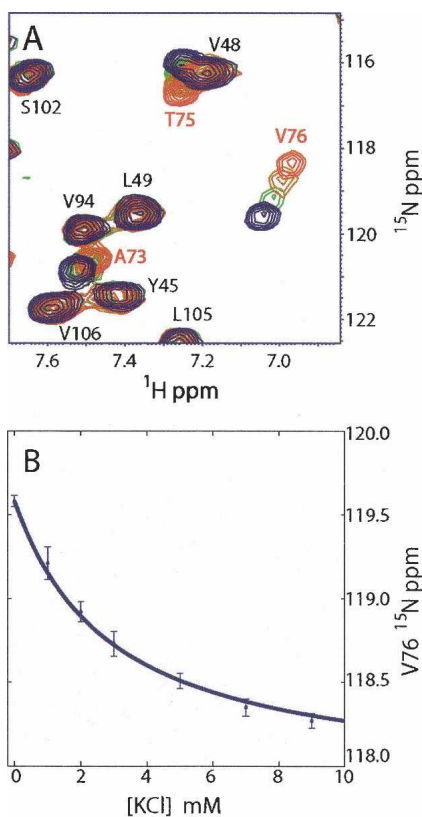


Figure 8. K^+ -titration of the KcsA channel in SDS micelles. (A) Region of the 1H - ^{15}N -tr-HSQC spectrum of tetrameric KcsA in 200 mM SDS and 25 mM MES (pH 6.0) in 99% D_2O acquired on a DRX800 spectrometer at 323 K. Spectra at 0, 1, 3, and 7 mM KCl are shown in blue, green, yellow, and red, respectively. Residues A73, T75, and V76 of the selectivity filter and its environment (red labels) exhibit chemical shift changes, while other residues (black labels) are unaffected by the change in K^+ concentration. (B) Titration curve following the chemical shift of the V76 backbone ^{15}N , which exhibits the largest K^+ -induced change. The best fitted curve assuming (to a first-order approximation) a bimolecular reaction between tetrameric channel and K^+ ion corresponds to a K_D of 3 ± 0.5 mM.

pH-induced chemical shift change as well. In both KcsA^E and KcsATM, the changes in backbone ^{13}C chemical shifts are relatively small, exhibiting RMS values of 0.2 and 0.1 ppm, respectively. The small nature of the chemical shift changes indicates that the KcsA time-averaged structure undergoes minimal change in the range of pH values studied.

Discussion

Large membrane proteins pose great difficulties for high-resolution NMR methods. Stringent demands are placed upon sample stability and global tumbling times, requiring extensive optimization of sample conditions. Because of the necessity for solubilization of the protein by detergent, correlation times are increased beyond

those expected for the naked protein, making the acquisition of triple-resonance spectra a challenging and time-consuming process. The protein of interest in this work, KcsA, presents attractive features as a target for structural studies, because as a heat-resistant homotetramer, its spectra are considerably simplified relative to single-chain proteins of the same size. On the other hand, it is also mostly helical, representing a class of proteins that typically exhibits less chemical shift dispersion and which often proves more difficult to NMR. In this work, we have shown backbone assignment to be possible for tetrameric KcsA in SDS micelles at 323 K, providing a stepping stone to study its structure and dynamics under different conditions, as well as its interaction with detergent molecules.

Comparison with KcsA structures

A comparison of our secondary chemical shift, amide proton NOE connectivities, and hydrogen-exchange NMR data with the crystal structure reported for residues 23–119 of KcsA (Doyle et al. 1998) reveals excellent agreement. The three previously identified structural elements of KcsA, the TM1, pore, and TM2 helices are located in the crystal structure at residues 27–51, 62–74, and 86–112. NMR C^α secondary chemical shifts identify these structural elements at residues 31–52, 62–73, and 86–115, respectively. The R²⁷AAGA³¹ segment preceding the TM1 helix shows slow HX rates and strong sequential amide NOEs, suggestive of a helical conformation for this region too. Ala and Gly residues within the transmembrane helices tend to have smaller ^{13}C secondary chemical shifts than other residues, possibly accounting for the modest secondary chemical shifts seen in this region. The unusually elevated apparent HX rate of residue T112 is likely to be an artifact resulting from OH-mediated intraresidue NOE attenuation.

The cytoplasmic N- and C-terminal segments of KcsA represent obvious putative sites for binding cellular factors that regulate channel opening. Therefore, structural elements in these regions are of great interest, particularly since previously they were removed in order to obtain sufficiently diffracting crystals. In a site-directed spin-labeling (SDSL) study of full-length KcsA (residues 1–160) in liposomes (Cortes et al. 2001), N-terminal residues (1–20) were found to form a helix that enters the membrane at residues 15–16 and is linked by a disordered loop of 5–6 residues to the TM1 domain. In our study, both secondary shifts and HX rates suggest that residues 16–19 form a helical turn, whereas the following residues are disordered. We conclude, therefore, that the helical character of native KcsA residues is preserved in our shorter construct. In contrast, SDSL and NMR data provide conflicting views regarding secondary structure

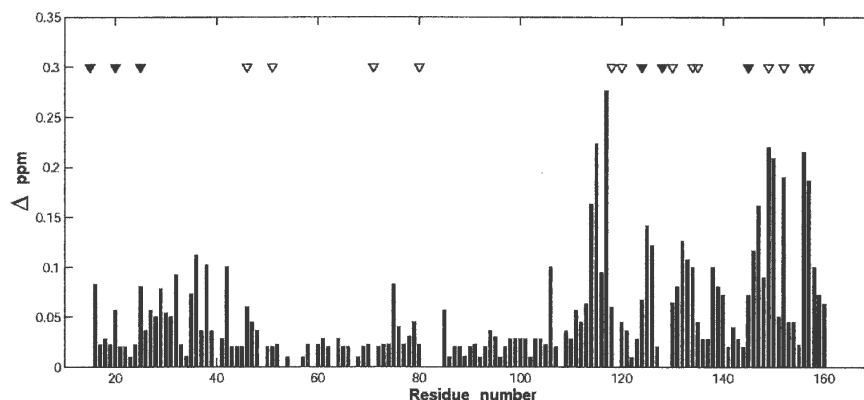


Figure 9. pH-induced changes in KcsA backbone chemical shifts. Chemical shifts of the ^1H - ^{15}N backbone moiety at pH 6.0 and 8.0 are compared. The y-axis represents a weighted change in chemical shift Δ , defined as $\Delta = \sqrt{(\delta_{\text{H}})^2 + (\delta_{\text{N}}/5)^2}$, with δ_{H} and δ_{N} representing the changes in chemical shift of amide ^1H and ^{15}N , respectively, between the two pH values. Experimental uncertainty in Δ is ≤ 0.01 ppm. Overhead triangular markers designate residues with pH-dependent electrostatic characteristics that may exert a local effect upon chemical shift. Dark triangles represent His residues (excluding the first five residues of the His₆ tag), and open triangles represent the acidic residues Asp and Glu. While the pK_a of the acidic residues is below five, this value may be elevated by the negatively charged headgroups of SDS, a possibility supported by the correlation between chemical shift change in the C-terminal domain and the location of these residues. Of the residues lacking a His/Asp/Glu neighbor, residues F114 and V115 represent the largest observed chemical shift change.

in the C-terminal domain. The spin-labeling study predicts the C-terminal region to contain two helical stretches, spanning residues 129–148 and 154–160, whereas our NMR data locate a single C-terminal helix at residues 142–155, and residues 124–137 and 156–160 appear to lack any significant structure. Notably, the SDSL study was performed at low pH (~ 4) and in liposomes, rather than a strongly anionic detergent. A recent study established structural differences between KcsA solubilized in native-like membranes and detergents (Encinar et al. 2005). Nevertheless, it is noteworthy that the sequence of the helical segment proposed in our NMR results is amphiphilic, making it conducive to the formation of a tetrameric helical bundle. In this assembly, residues L144, F148, L151, M154, and L155 would create the hydrophobic surface of the helix facing inward to the fourfold symmetry axis. R147 is the only residue opposing such an arrangement, but it is conceivable that with moderate distortions in the helices, its relatively long side chain allows the guanidino group to reach the solvent. The opposite face of the helix is rich in charged Asp and Arg residues, which could stabilize this region in the aqueous environment. Although we cannot unambiguously establish the presence of a tetrameric arrangement for the C-terminal helix from the data at hand, we would expect lower transverse ^{15}N relaxation rates than observed for this helix and the unstructured region preceding the helix if it were monomeric. Therefore, our results appear more compatible with at least partial occupation of a parallel four-helical bundle arrangement.

Residue-specific modulation of secondary chemical shifts in the membrane environment

With the increasing available volume of backbone ^{13}C chemical shift data for proteins, secondary chemical shifts are a primary source of structural information used in numerous structure determination algorithms (Kuszewski et al. 1995; Cornilescu et al. 1999; Wishart 2001). However, data on the behavior of chemical shifts in membrane proteins lags behind the abundant information available for their soluble counterparts. The backbone assignment of KcsA helps to address this paucity of data. Although based upon limited data (a total of 60 residues), a characteristic pattern of residue-specific secondary shift magnitudes appears evident. This is best appreciated by comparing $^{13}\text{C}^{\alpha}$ chemical shifts in the three buried KcsA helices to average helical values (as opposed to random coil values) (Zhang et al. 2003). Analysis shows that the largest deviations are observed for the β -OH-substituted residues Ser (3) and Thr (4), averaging downfield shifts of 2.4 and 1.2 ppm, respectively, and the β -branched residues Ile (2) and Val (12), averaging downfield shifts of 1.6 and 0.9 ppm (the number of averaged residues appears in parentheses). Similar effects are observed when analyzing the chemical shifts of the transmembrane helical residues in diacylglycerol kinase (DAGK) (Oxenoid et al. 2004).

Notably, the four amino acids whose chemical shifts are most affected in membrane helices also experience the largest downfield shift when moving from random coil to helical conformation (Zhang et al. 2003). This

suggests that the lipophilic environment is amplifying effects exerted upon helices in soluble proteins as well. Formation of hydrogen bonds between β -OH groups and the carbonyl in the preceding turn of the helix is favored in both aqueous (Gray and Matthews 1984) and membrane-spanning (Chamberlain and Bowie 2004) α -helices. We propose that as this interaction becomes more dominant in the lipophilic environment, the resulting equilibrium shift accentuates the “helicity effect” and accounts for the larger downfield deviation observed. This consideration also correctly predicts a more pronounced effect upon Ser compared with Thr residues. Since the Ser side chain, lacking the β -substituent, would have more conformational freedom prior to the formation of the β -OH hydrogen bond, the relative effect of the hydrophobic environment upon its chemical shift would be greater.

Cross-relaxation effects and structural characterization of SDS–KcsA mixed micelles

Detergents and lipids are an inseparable part of membrane protein structure. Previous structural studies have focused upon this key participant in the membrane protein assembly by monitoring the appearance of NOESY cross-peaks between various detergent and protein protons (Fernández et al. 2002; Rooslid et al. 2005), the relaxation-enhancing effects of spin-labeled detergent molecules (Hilty et al. 2004), or estimating detergent–protein cross-relaxation (Ulmer and Bax 2005). Here, we study the assembly of SDS molecules around the KcsA tetramer by following the attenuation of amide proton signals resulting from an inversion of specific detergent proton populations. The slow NOE buildup between SDS and KcsA implies that while effective correlation times τ_{int} for the SDS–KcsA interaction are longer than the $\omega\tau_{\text{int}} = 1$ limit ($\tau_{\text{int}} > 200$ psec), they are much shorter than the overall tumbling time of the KcsA-containing micelle. Notably, the NMR spectrum shows narrow SDS resonances, with relaxation properties not measurably affected by the KcsA, indicative of rapid exchange between monomeric SDS, free SDS micelles, and KcsA-containing micelles. The detergent must therefore be treated as a highly fluid medium, and NOE attenuations are a function of both the occupancy and residence time of detergent at the protein interface. In contrast, intraprotein NOEs between amide protons are governed by the long protein τ_{C} and build up far more rapidly, particularly in helical domains, and result in spin diffusion. The slow SDS–KcsA NOE buildup makes the use of short mixing times (≤ 20 msec) that would avoid such spin diffusion impractical. Intraprotein NOEs account for the comparable attenuation observed for the two TM domains. Although the “inner” helix (TM2) is less exposed to the environment, one in every three to four

residues does interact with detergent protons, and the attenuation then rapidly propagates by spin diffusion in the slow tumbling KcsATM domain. Since the relation $\tau_{\text{int}} \ll \tau_{\text{C}}$ generally holds for large membrane proteins, protein–detergent NOES may be better suited for mapping the exposure of protein segments, rather than particular residues, to detergent.

Despite these limitations, a clear structural picture emerges from our results. The data in Figure 7 can be explained by a population of SDS molecules oriented parallel (or antiparallel) to the TM helices, “hugging” the surface of the membrane-spanning domains. This would account for the observed distribution of C^2H_2 - and C^{12}H_3 -induced attenuations along the TM domains. In fast exchange with this population must be additional SDS molecules oriented perpendicularly to the channel fourfold axis, with their hydrophobic tails contacting KcsA, since two SDS molecules fail to span the entire membrane (Fig. 10). In this hemitoroidal arrangement, the micelle optimally covers the surface of KcsA, while the interface between the hydrophobic detergent molecules and the aqueous environment is minimized. To relate this macromolecular assembly with the physical parameters of KcsA, we model the channel as an open-ended cone, with a height of 34 Å and base diameters of 47 Å and 25 Å for the extracellular and cytoplasmic sides, respectively. These dimensions include an additional 2 Å on either side of the backbone to account for the spatial requirements of the hydrophobic side chains. Assuming the SDS hydrocarbon

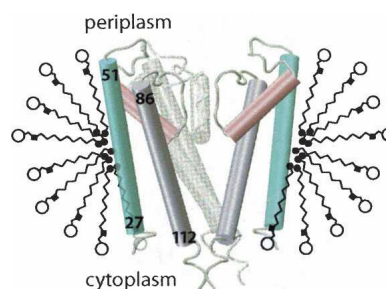


Figure 10. Assembly of the KcsA-containing SDS micelle as suggested by cross-relaxation attenuation maps. Shown is a cross-section through the KcsA-containing SDS micelle defined by the pore helices of two diametrically opposed KcsA subunits. The TM1 (residues 27–51), TM2 (residues 86–112), and pore helices (residues 62–74, numbers not shown) of the emphasized subunits are shown in light blue, purple, and pink, respectively. The distant subunit is shown in gray, and the front subunit is omitted for clarity. SDS molecules (drawn to scale) are black, with the anionic head groups represented by large open circles, and the C^2 and C^{12} carbons highlighted as filled squares and circles, respectively. Attenuation originating from inversion of C^{12} protons is most significant for KcsA residues at the center of the TM1 and TM2 helices, and the C-terminal end of the pore helix. Attenuation originating from inversion of C^2 protons is most pronounced for residues of the pore helix and for residues at both ends of the TM helices.

chains occupy a cylinder 16 Å long and with a 4.3 Å diameter, we calculate that ~190 SDS molecules are required to fulfill the hydrophobic requirements of KcsA, and estimate the total micellar molecular weight at ~122 kDa. This number agrees well with the results of DLS measurements, which predict a molecular weight of 115 ± 10 kDa, as well as the KcsATM correlation time of 40 nsec at 323 K, which corresponds to a molecular weight of ~120 kDa.

Conformational changes associated with gating in KcsA

The pH dependence of ion conductance through the potassium channel has been a heatedly debated subject in recent years (Cuello et al. 1998; Heginbotham et al. 1999; Zakharian and Reusch 2004). The biological significance of a pH-gating mechanism is not clear, in view of the fact that intracellular pH must be closely controlled (Corvini et al. 2000). It is assumed that the pH change mimics the action of a cellular effector, which binds to the cytoplasmic domain of the channel. Since KcsATM is devoid of residues with pH-dependent electrostatic characteristics, and presumably insulated by the hydrophobic interior of the micelle from the macroscopic pH, changes in chemical shift clustered in the TM1 helix may reflect structural differences between high- and low-pH states of the channel. Notably, some—but not all—of the changes observed when moving from pH 8 to pH 6 are echoed in the KCl-titration. This suggests the K⁺- and pH-induced changes in KcsATM and the selectivity filter may be structurally related.

Because of their unique side-chain pKa, histidine residues are often involved in pH-dependent conformational changes. The crystal structure of KcsA^{23–119} (Doyle et al. 1998) suggests a single possible long-range histidine interaction, residue H25, which precedes the TM1 domain packing against residues 114–118 at the base of the TM2 helix of the adjacent subunit. This segment has been postulated to represent a binding site for cellular modulators of channel activity (Cortes et al. 2001). Indeed, chemical shift changes in this segment represent the only effect observed in the C-terminal region unaccounted for by local electrostatic changes. The NMR data suggest that conformational changes at the convergence of the four subunits could be propagated to the TM1 helix and influence the flux of K⁺ ions through the channel by a mechanism yet to be uncovered. Although chemical shift changes in TM1 are not consistent with a large-scale conformational change in KcsA, it should be noted that we have not monitored these changes at lower pH values, since SDS-solubilized tetrameric KcsA loses its thermostability at such conditions. Chemical shift changes at pH 6 may therefore reflect only a small alteration in the equilibrium between two channel states, merely

hinting at the magnitude of the effect expected when the channel moves to a fully open state.

Materials and methods

Expression and purification of KcsA

The forward primer 5'-CACCCATATGCATCATCATCATC ATCATCTTCTG-GGCCGTCACGG and reverse primer 5'-GGATCCTCATTATTAACGACGGTTATC-GTCAAGC ATACGTTCCAGACGG were used to amplify the region encoding amino acids 16–160 of KcsA (sequence numbering follows Doyle et al. 1998) and cloned into pET100/D-TOPO vector (Invitrogen). Subsequently, the insert was isolated by digestion with NdeI and BamHI restriction endonucleases and cloned into pET11a vector (Novagen). The resulting construct containing a 6-histidine tag preceding the N terminus of KcsA^{16–160} was verified both by DNA sequencing and mass spectrometry.

Expression of KcsA followed general guidelines previously proposed (Gardner and Kay 1998). OverExpress C41(DE3) *Escherichia coli* cells (Avidis) (Miroux and Walker 1996) containing the KcsA plasmid were cultured in a modified M9 medium (Cai et al. 1998) at 37°C until an OD₆₀₀ of 0.6 was reached. Cells were then transferred into a D₂O-based M9 medium containing 4 g/L ¹³C-glucose and supplemented with 1 g/L ²H, ¹³C, ¹⁵N-labeled Isotec medium (Sigma-Aldrich) and grown to OD₆₀₀ of 0.8. Isopropylthiogalactoside (IPTG) was added to a final concentration of 1 mM and shaking was continued for 16 h at 27°C. For expression of KcsA with amide protonation in the transmembrane domains (KcsATM), the D₂O-based medium was replaced by a glucose-deficient H₂O-based M9 medium containing 4–7 g/L ²H, ¹³C, ¹⁵N-labeled Isogro medium (Isotec).

Purification of tetrameric KcsA followed the general protocol previously outlined by Shimada and coworkers (Takeuchi et al. 2003) with minor modifications. After harvesting, cells were lysed by sonication in buffer containing 20 mM Tris (pH 8), 150 mM KCl, 150 mM NaCl, 20 mM imidazole, and 5 mM benzamidine. KcsA was extracted for 60–90 min at 4°C using 20 mM DM, and the suspension was clarified by centrifugation. The supernatant was loaded on a Ni⁺⁺-charged HiTrap Chelate column (Amersham Biosciences) and eluted using 400 mM imidazole in Tris (pH 8) buffer containing 5 mM DM. KcsA was concentrated to 1–1.5 mL in a Centriprep YM10 device (Millipore) and fractionated on a size-exclusion column (Superdex 200 16/60, Amersham Biosciences) equilibrated with 25 mM N-morpholino-ethane-sulfonate (MES) buffer at pH 6.0 (20 mM Tris at pH 8.0 for samples at pH 8) and 10 mM sodium dodecyl sulfate (SDS). For preparation of samples in other detergents, KcsA in SDS buffer was pooled and concentrated before reloading again on the same size-exclusion column, equilibrated with appropriate buffer and appropriate detergent. KcsA in SDS micelles was concentrated using Centriprep and Amicon Ultra devices (Millipore) to volumes of 300–700 μL for NMR measurements.

Sample preparation

NMR measurements were recorded at concentrations of 0.25–0.35 mM tetrameric KcsA (1.0–1.4 mM monomeric concentration) in 25 mM MES (pH 6.0) or 20 mM Tris (pH 8.0) and a

100–200:1 excess of detergent over monomer. Samples with amide protonation in the solvent-accessible domains (KcsA^E) were prepared in 93% H₂O, 7% D₂O. Samples with amide protonation in the transmembrane domains (KcsATM) were lyophilized once and dissolved in 99.9% D₂O.

NMR measurements

All NMR measurements were conducted at 323 K. Sample stability at elevated temperatures was verified using SDS–polyacrylamide gels and by NMR. Data were collected on DRX600 and DRX800 Bruker spectrometers using cryogenic triple-resonance probeheads equipped with z-axis pulsed field gradients. Triple resonance, TROSY versions (Salzmann et al. 1998) of the HNCO, HN(CO)CA, HN(CA)CO, and HNCA experiments for purposes of backbone assignment were carried out for ²H, ¹³C, ¹⁵N-labeled KcsA^E at 600 MHz field using a TROSY (tr) block similar to that suggested by Pervushin and coworkers (Pervushin et al. 1998) optimized for water suppression on cryoprobes (A. Bax, unpubl.). Triple-resonance experiments were typically acquired with 32–36 complex points and an acquisition time of 20.2–22.8 msec in the ¹⁵N dimension, and 512 complex points and an acquisition time of 63.2 msec in the observed dimension. Experiments with ¹³CO (¹³Cα) evolution were acquired with 32–40 complex points and 21.2–26.5 (7–7.5) msec acquisition time. 3D ¹H-¹⁵N NOESY-HMQC and ¹⁵N HMQC-NOESY-HMQC spectra were acquired at 800 MHz field with mixing times of 70–80 (250) msec for KcsATM (KcsA^E) samples, respectively. These were acquired with 40–50 complex points and an acquisition time of 19–23.7 msec in the ¹⁵N {F2} dimension, and 512 complex points and an acquisition time of 45.9 msec in the observed dimension. Experiments with ¹H^N (¹⁵N) evolution were acquired with 72 (50) complex points and an acquisition time of 13.6 (23.6) msec. NOESY experiments utilized a selective E-BURP first ¹H pulse to minimize excitation of solvent and detergent protons.

To overcome the poor dispersion of ¹H-¹⁵N signals for KcsA^E, protein–detergent NOE attenuations and hydrogen-exchange rates were measured using three-dimensional tr-HNCO-based experiments. In the case of protein–detergent dipolar interactions, SDS protons were selectively inverted using an IBURP2 sequence (Geen and Freeman 1991) and a 40-msec selective pulse, and allowed a 50–250 msec mixing time preceding the tr-HNCO sequence. This was repeated for each of the four distinct proton chemical shifts in the 1D spectrum of SDS. The SDS-to-protein NOE effect increases steadily with mixing time, and the highest signal-to-noise data, collected at 250 msec, were used for analysis. For estimating hydrogen-exchange rates of SDS-KcsA in 20 mM Tris (pH 8.0), the H₂O protons were selectively inverted prior to the tr-HNCO sequence, with radiation damping suppressed using a weak 1 G/cm gradient throughout a mixing time of 25 msec. In all experiments, a reference spectrum, in which the inversion pulse was replaced by an appropriate delay, was acquired in interleaved fashion, and care was taken to purge steady-state ¹⁵N magnetization.

K⁺-titration of KcsA was performed by successively adding aliquots of a 50 mM KCl solution in 100 mM MES (pH 6.0) in 99.9% D₂O to a NMR sample of 0.18 mM tetrameric KcsA (determined by absorbance at 280 nm) in 200 mM SDS and 25 mM MES (pH 6.0) in 99% D₂O. A ¹H-¹⁵N-tr-HSQC (108 complex points and 50-msec acquisition time in the ¹⁵N dimension, total measurement time of 100 min.) was acquired at K⁺ concentrations of 0–9 mM on a DRX800 Bruker spectrometer

at 323 K. Peak position for the amide ¹⁵N of residue V76 was used to estimate the K⁺-binding constant.

Data analysis

In all NMR experiments, FIDs were weighted by sine square and sine functions (both shifted 72° and truncated at 168°), in acquisition and evolution dimensions, respectively, and Fourier transformed. All spectra were processed and examined using the NMRPipe/NMRDraw software package (Delaglio et al. 1995). Backbone assignment was performed with the aid of in-house scripts. The dipolar interaction between protein and detergent protons was qualitatively assessed using the ratio of tr-HNCO peaks in the interleaved inversion and reference spectra. Solvent exchange rates for amide protons were estimated in a similar fashion, and this intensity ratio was used to calculate exchange rates assuming a mono-exponential recovery curve.

CD measurements

CD spectra of KcsA (at 25 μM monomeric concentration) were recorded in various buffer/detergent mixtures on a JASCO J-700 spectropolarimeter using a 0.05-cm path length cell at 25°C. Quantitative evaluation of secondary structure from the CD spectrum was carried out using the program CDNN (www.bioinformatik.bio-chemtech.uni-halle.de/cd_spect/index.html).

Dynamic light scattering measurements

Light scattering data were obtained using an analytical Superdex-200 column 10/30 (Amersham Biosciences) with in-line multiangle light scattering (DAWN EOS, Wyatt Technology, Inc.) and refractive index detectors (OPTILAB DSP, Wyatt Technology, Inc.) and processed using the Astra V 5.1.3.0 software. Samples of 150–300 μg of protein in 125 μL of either 20 mM Tris-HCl (pH 8) or 25 mM sodium phosphate (pH 6) containing 10 mM SDS were applied to the pre-equilibrated S200 column running at a flow rate of 0.5 mL/min at room temperature and eluted with the same buffer.

Acknowledgments

We thank Annie Aniana for expert technical assistance, Ichio Shimada (University of Tokyo) for the KcsA purification protocol, Frank Delaglio for software support, and Vitali Tugarinov (University of Toronto) for helpful comments. J.H.C. acknowledges the support of a long-term EMBO fellowship. This work was supported by the Intramural Research Program of the NIDDK, NIH, and by the Intramural AIDS-Targeted Antiviral Program of the Office of the Director, NIH.

References

- Arora, A. and Tamm, L.K. 2001. Biophysical approaches to membrane protein structure determination. *Curr. Opin. Struct. Biol.* **11**: 540–547.
- Arora, A., Abildgaard, F., Bushweller, J.H., and Tamm, L.K. 2001. Structure of outer membrane protein A transmembrane domain by NMR spectroscopy. *Nat. Struct. Biol.* **8**: 334–338.

- Bax, A. and Grzesiek, S. 1993. Methodological advances in protein NMR. *Acc. Chem. Res.* **26**: 131–138.
- Cai, M., Huang, Y., Sakaguchi, K., Clore, G.M., Gronenborn, A.M., and Craigie, R. 1998. An efficient and cost-effective isotope labeling protocol for proteins expressed in *Escherichia coli*. *J. Biomol. NMR* **11**: 97–102.
- Chamberlain, A.K. and Bowie, J.U. 2004. Analysis of side-chain rotamers in transmembrane proteins. *Biophys. J.* **87**: 3460–3469.
- Cornilescu, G., Delaglio, F., and Bax, A. 1999. Protein backbone angle constraints from searching a database for chemical shift and sequence homology. *J. Biomol. NMR* **13**: 289–302.
- Cortes, D.M., Cuello, L.G., and Perozo, E. 2001. Molecular architecture of full-length KcsA: Role of cytoplasmic domains in ion permeation and activation gating. *J. Gen. Physiol.* **117**: 165–180.
- Corvini, P.F., Gautier, H., Rondags, E., Vivier, H., Goergen, J.L., and Germain, P. 2000. Intracellular pH determination of pristinamycin-producing *Streptomyces pristinaespiralis* by image analysis. *Microbiol.* **146**: 2671–2678.
- Cuello, L.G., Romero, J.G., Cortes, D.M., and Perozo, E. 1998. pH-dependent gating in the *Streptomyces lividans* K⁺ channel. *Biochemistry* **37**: 3229–3236.
- Delaglio, F., Grzesiek, S., Vuister, G.W., Zhu, G., Pfeifer, J., and Bax, A. 1995. NMRPipe: A multidimensional spectral processing system based on UNIX pipes. *J. Biomol. NMR* **6**: 277–293.
- Doyle, D.A., Cabral, J.M., Pfuetzner, R.A., Kuo, A., Gulbis, J.M., Cohen, S.L., Chait, B.T., and MacKinnon, R. 1998. The structure of the potassium channel: Molecular basis of K⁺ conduction and selectivity. *Science* **280**: 69–77.
- Encinar, J.A., Molina, M.L., Poveda, J.A., Barrera, F.N., Renart, M.L., Fernandez, A.M., and Gonzalez-Ros, J.M. 2005. The influence of a membrane environment on the structure and stability of a prokaryotic potassium channel KcsA. *FEBS Lett.* **579**: 5199–5204.
- Ferentz, A.E. and Wagner, G. 2000. NMR spectroscopy: A multifaceted approach to macromolecular structure. *Q. Rev. Biophys.* **33**: 29–65.
- Fernández, C. and Wüthrich, K. 2003. NMR solution structure determination of membrane proteins reconstituted in detergent micelles. *FEBS Lett.* **555**: 144–150.
- Fernández, C., Hilty, C., Wider, G., and Wüthrich, K. 2002. Lipid-protein interactions in DHPC micelles containing the integral membrane protein OmpX investigated by NMR spectroscopy. *Proc. Natl. Acad. Sci.* **99**: 13533–13537.
- Frueh, D.P., Ito, T., Li, T.S., Wagner, G., Glaser, S.J., and Khaneja, N. 2005. Sensitivity enhancement in NMR of macromolecules by application of optimal control theory. *J. Biomol. NMR* **32**: 23–30.
- Fu, R. and Cross, T.A. 1999. Solid-state nuclear magnetic resonance investigation of protein and polypeptide structure. *Annu. Rev. Biophys. Biomol. Struct.* **28**: 235–268.
- Gardner, K.H. and Kay, L.E. 1998. The use of ²H, ¹³C, ¹⁵N multidimensional NMR to study the structure and dynamics of proteins. *Annu. Rev. Biophys. Biomol. Struct.* **27**: 357–406.
- Geen, H. and Freeman, R. 1991. Band-selective radiofrequency pulses. *J. Magn. Reson.* **93**: 93–141.
- Gray, T.M. and Matthews, B.W. 1984. Intrahelical hydrogen bonding of serine, threonine and cysteine residues within α -helices and its relevance to membrane-bound proteins. *J. Mol. Biol.* **175**: 75–81.
- Grzesiek, S., Anglister, J., Ren, H., and Bax, A. 1993. ¹³C line-narrowing by ²H decoupling in ²H/¹³C/¹⁵N enriched proteins. Application to triple resonance 4D J-connectivity of sequential amides. *J. Am. Chem. Soc.* **115**: 4369–4370.
- Gulbis, J.M. and Doyle, D.A. 2004. Potassium channel structures: Do they conform? *Curr. Opin. Struct. Biol.* **14**: 440–446.
- Heginbotham, L., Lu, Z., Abramson, T., and MacKinnon, R. 1994. Mutations in the K⁺ channel signature sequence. *Biophys. J.* **66**: 1061–1067.
- Heginbotham, L., Odessey, E., and Miller, C. 1997. Tetrameric stoichiometry of a prokaryotic K⁺ channel. *Biochemistry* **36**: 10335–10342.
- Heginbotham, L., LeMasurier, M., Kolmakova-Partensky, L., and Miller, C. 1999. Single streptomyces lividans K⁺ channels: Functional asymmetries sidedness of proton activation. *J. Gen. Physiol.* **114**: 551–559.
- Hille, B. 2001. *Ion channels of excitable membranes*, 3rd ed. Sinauer Associates, Sunderland, MA.
- Hilty, C., Wider, G., Fernández, C., and Wüthrich, K. 2004. Membrane protein-lipid interactions in mixed micelles studied by NMR spectroscopy with the use of paramagnetic reagents. *Chembiochem.* **5**: 467–473.
- Ho, K., Nichols, C.G., Lederer, W.J., Lytton, J., Vassiliev, P.M., Kanazirska, M.V., and Herbert, S.C. 1993. Cloning and expression of an inwardly rectifying ATP-regulated potassium channel. *Nature* **362**: 31–38.
- Hwang, P.M., Choy, W.-Y., Lo, E.I., Forman-Kay, J.D., Raetz, C.R.H., Prive, G.G., Bishop, R.E., and Kay, L.E. 2002. Solution structure and dynamics of the outer membrane enzyme PagP by NMR. *Proc. Natl. Acad. Sci.* **99**: 13560–13565.
- Jiang, Y., Lee, A., Chen, J., Ruta, V., Cadene, M., Chait, B.T., and MacKinnon, R. 2003. X-ray structure of a voltage-dependent K⁺ channel. *Nature* **423**: 33–41.
- Jiang, Y., Wang, D.N., and MacKinnon, R. 2004. Electron microscopic analysis of KvAP voltage-dependent K⁺ channels in an open conformation. *Nature* **430**: 806–810.
- Kuo, A., Gulbis, J.M., Antcliff, J.F., Rahman, T., Lowe, E.D., Zimmer, J., Cuthbertson, J., Ashcroft, F.M., Ezaki, T., and Doyle, D.A. 2003. Crystal structure of the potassium channel KirBac1.1 in the closed state. *Science* **300**: 1922–1926.
- Kuszewski, J., Qin, J., Gronenborn, A.M., and Clore, G.M. 1995. The impact of direct refinement against ¹³C α and ¹³C β chemical shifts on protein structure determination by NMR. *J. Magn. Reson. B* **106**: 92–96.
- LeMasurier, M., Heginbotham, L., and Miller, C. 2001. KcsA: It's a potassium channel. *J. Gen. Physiol.* **118**: 303–313.
- Lohr, F., Kastemi, V., Hartleib, J., Gunther, U., and Ruterjans, H. 2003. A strategy to obtain backbone resonance assignments of deuterated proteins in the presence of incomplete amide ²H/¹H back-exchange. *J. Biomol. NMR* **25**: 291–311.
- MacKinnon, R. 2003. Potassium channels. *FEBS Lett.* **555**: 62–65.
- Maity, H., Lim, W.-K., Rumbley, J.N., and Englander, S.W. 2003. Protein hydrogen exchange mechanism: Local fluctuations. *Protein Sci.* **12**: 153–160.
- Marassi, F.M., Gessell, J.J., and Opella, S.J. 1999. Recent developments in multidimensional NMR methods for structural studies of membrane proteins. In *Biological magnetic resonance*, Vol. 16 (eds. N.R. Krishna and L.J. Berliner), pp. 121–145. Kluwer Academic/Plenum Publishers, New York.
- Mesleh, M.F., Lee, S., Veglia, G., Thiriot, D.S., Marassi, F.M., and Opella, S.J. 2003. Dipolar waves map the structure and topology of helices in membrane proteins. *J. Am. Chem. Soc.* **125**: 8928–8935.
- Miller, C. 2000. An overview of the potassium channel family. *Genome Biol.* **1**: 1–5.
- Miroux, B. and Walker, J.E. 1996. Over-production of proteins in *Escherichia coli*: Mutant hosts that allow synthesis of some membrane proteins and globular proteins at high levels. *J. Mol. Biol.* **260**: 289–298.
- Molina, M.L., Encinar, J.A., Barrera, F.N., Fernandez-Ballester, G., Riquelme, G., and Gonzalez-Ros, J.M. 2004. Influence of C-terminal protein domains and protein-lipid interactions on tetramerization and stability of the potassium channel KcsA. *Biochemistry* **43**: 14924–14931.
- Oxenoid, K. and Chou, J.J. 2005. The structure of phospholamban pentamer reveals a channel-like architecture in membranes. *Proc. Natl. Acad. Sci.* **102**: 10870–10875.
- Oxenoid, K., Kim, H.J., Jason, J., Sonnichsen, F.D., and Sanders, C.R. 2004. NMR assignments for a helical 40 kDa membrane protein. *J. Am. Chem. Soc.* **126**: 5048–5049.
- Pervushin, K.V., Riek, R., Wider, G., and Wüthrich, K. 1997. Attenuated T₂ relaxation by mutual cancellation of dipole-dipole coupling and chemical shift anisotropy indicates an avenue to NMR structures of very large biological macromolecules in solution. *Proc. Natl. Acad. Sci.* **94**: 12366–12371.
- Pervushin, K.V., Wider, G., and Wüthrich, K. 1998. Single-transition to single-transition polarization transfer (ST2-PT) in [¹⁵N,¹H]-TROSY. *J. Biomol. NMR* **12**: 345–348.
- Pongs, O., Kecskemethy, N., Muller, R., Krah-Jentgens, I., Baumann, A., Kiltz, H.H., Canal, I., Llamazares, S., and Ferrus, A. 1988. Shaker encodes a family of putative potassium channel proteins in the nervous system of *Drosophila*. *EMBO J.* **7**: 1087–1096.
- Riek, R., Fiaux, J., Bertelsen, F.B., Horwich, A.L., and Wüthrich, K. 2002. Solution NMR techniques for large molecular and supramolecular structures. *J. Am. Chem. Soc.* **124**: 144–153.
- Rooslid, T.P., Greenwald, J., Vega, M., Castronovo, S., Riek, R., and Choe, S. 2005. NMR structure of Mistic, a membrane-integrating protein for membrane protein expression. *Science* **307**: 1317–1321.
- Salzmann, M., Pervushin, K., Wider, G., Senn, H., and Wüthrich, K. 1998. TROSY in triple-resonance experiments: New perspectives for sequential NMR assignment of large proteins. *Proc. Natl. Acad. Sci.* **95**: 13585–13590.
- Takeuchi, K., Yokogawa, M., Matsuda, T., Sugai, M., Kawano, S., Kohno, T., Nakamura, H., Takahashi, H., and Shimada, I. 2003. Structural basis of the KcsA K⁺ channel and agitoxin2 pore-blocking

- toxin interaction by using the transferred cross-saturation method. *Structure* **11**: 1381–1392.
- Tugarinov, V., Muhandiram, R., Ayed, A., and Kay, L.E. 2002. Four-dimensional NMR spectroscopy of a 723-residue protein: Chemical shift assignments and secondary structure of malate synthase G. *J. Am. Chem. Soc.* **124**: 10025–10035.
- Tugarinov, V., Hwang, P.M., and Kay, L.E. 2004. Nuclear magnetic resonance spectroscopy of high-molecular-weight proteins. *Annu. Rev. Biochem.* **73**: 107–146.
- Ulmer, T.S. and Bax, A. 2005. Comparison of structure and dynamics of micelle-bound human α -synuclein and Parkinson disease variants. *J. Biol. Chem.* **280**: 43179–43187.
- Valiyaveetil, F.I., Zhou, Y., and MacKinnon, R. 2002. Lipids in the structure, folding and function of the KcsA K^+ channel. *Biochemistry* **41**: 10771–10777.
- Wand, A.J. and Englander, S.W. 1996. Protein complexes studied by NMR spectroscopy. *Curr. Opin. Biotechnol.* **4**: 403–408.
- Wider, G. 2005. NMR techniques used with very large biological macromolecules in solution. *Methods Enzymol.* **394**: 382–398.
- Wishart, D.S. 2001. Use of chemical shifts in macromolecular structure determination. *Methods Enzymol.* **338**: 3–34.
- Zakharian, E. and Reusch, R.N. 2004. *Streptomyces lividans* potassium channel KcsA is regulated by the potassium electrochemical gradient. *Biochem. Biophys. Res. Commun.* **316**: 429–436.
- Zhang, H., Neal, S., and Wishart, D.S. 2003. RefDB: A database of uniformly referenced protein chemical shifts. *J. Biomol. NMR* **25**: 173–195.
- Zhou, Y. and MacKinnon, R. 2003. The occupancy of ions in the K^+ selectivity filter: Charge balance and coupling of ion binding to a protein conformational change underlie high conduction rates. *J. Mol. Biol.* **333**: 965–975.
- Zhou, Y., Morais-Cabral, J.H., Kaufmann, A., and MacKinnon, R. 2001. Chemistry of ion coordination and hydration revealed by a K^+ channel–Fab complex at 2.0 Å resolution. *Nature* **414**: 43–48.